Exchange integrals of commensurate and incommensurate structures of MFe_4Al_8 (M = U, Sc)

K. REĆKO
Faculty of Physics, University of Bialystok, K. Ciołkowskiego 1L, 15-245 Białystok, Poland

The appearance of the commensurability of UFe_4Al_8 alloy considering incommensurability of $ScFe_4Al_8$ compound is analysed on the basis of Heisenberg Hamiltonian. The influence of Dzyaloshinskii – Moriya and Ruderman-Kittel-Kasuya-Yoshida as well as the dipolar interactions as the main reasons of the noncollinearity and incommensurability of the alloys belonging to $ThMn_{12}$ family is investigated. The values and directions of the spin ordering found by magnetic diffraction are compared to that one's deriving from grand state configurations obtained by a simulated annealing algorithm. The lock-in magnetic modulations due to substitution of scandium by uranium atoms is discussed based on an appropriate exchange constants ratios.

(Received May 7, 2015; accepted September 9, 2015)

Keywords: 27.90+b Actinides, 72.80.Ga Transition-metal compounds, 75.30.Et Exchange interactions, 75.30.Gw Magnetic anisotropy

1. Introduction

The compounds with the general formula $M(FeAl)_{12}$ (M = Ac, Sc) crystallize in the body centred tetragonal system [1-4]. They form family showing a variety of magnetic structures, and in consequence a diversity of physical properties. In this paper, I consider the origin of the complex magnetic ordering which deals with MFe_4Al_8 crystallizing in a tetragonal structure of $ThMn_{12}$ – type. The system of interest has four independent high-symmetry sites. The crystal structure of MFe_4Al_8 with I 4/mmm symmetry and cell parameters a~860 pm, c~500 pm contains: 2(a) positions – occupied by magnetic M=U or paramagnetic M=Sc metal, (8f) – magnetic site, and 8(j), 8(i) – non–magnetic sites formed by Al atoms (see Fig.1). Except the occupation of the 2(a) and 8(f) positions, the occupation of the reminding positions does not depend on the f-electron or scandium component. Moreover, aluminium atoms which enter the 8(i) positions are these most stabilizing crystal structure [5] while saturation magnetic moment per formula unit for UFe_xAl_{12-x} systems disclose for iron content x=4 the strongest decrease [6]. The crystal structures of $ThMn_{12}$-type are layered systems, which suggest a strong anisotropy of the physical properties. Comparing the room temperature structural parameters and atomic radius of the (2a) resident at $ScFe_4Al_8$ alloy: a=860.2 pm, c=499.8 pm (r_{Sc} = 164 pm) [7] with typical for UFe_4Al_8 ones: a=873.65 pm, c=503.02 pm (r_U = 138 pm) [3, 8] it is obvious that scandium sample discloses significantly shorter interatomic distances with regard to distances at uranium one.

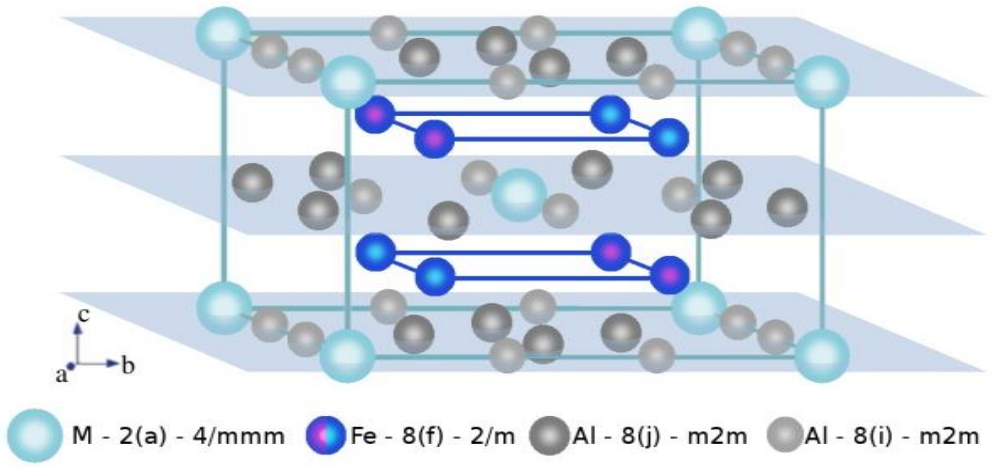

Fig.1 Sandwich construction of the crystal unit cell of the body centred tetragonal MFe_4Al_8 structure with in blue marked all potential magnetic sublattices

Obviously, magnetism occurs in these materials because of the presence of two kinds magnetic atoms namely *d*- and *f*-electronic. Their magnetic moments couple to one another and form magnetic order. Such coupling is

known as the exchange interaction and is rooted in the overlap of electrons in conjunction with Pauli's exclusion principle. Direct exchange operates between moments, which are close enough to have sufficient overlap of their wave functions. It gives a strong but short range coupling. When the atoms are very close together the Coulomb interaction is minimal when the electrons spend most of their time in between the nuclei. Since the electrons are then required to be at the same place in space at the same time, Pauli's exclusion principle requires that they possess opposite spins. According to Bethe and Slater the electrons spend most of their time between neighboring atoms when the interatomic distance is small. This gives rise to antiparallel alignment and therefore negative exchange. If the atoms are far apart the electrons spend their time away from each other in order to minimize the electron-electron repulsion. This gives rise to parallel alignment and positive exchange.

Considering the magnetic ordering along $[110]$ or $[1\bar{1}0]$ diagonals (see Fig.1) separately, it can be easy seen two iron collinear and ferromagnetic sublattices coupled antiferromagnetically each other with the third collinear and ferromagnetic – uranium site at uranium alloy, while the scandium sample consists of similar to uranium position the scandium ones with the antiferromagnetically coupled one collinear and the other one non-collinear ferromagnetic iron sublattice. Due to 1) the dominant coupling is an antiferromagnetic type, 2) similarity to so-called spin-canted structures and 3) the fact that the exchange interactions remain the distance function, the appropriate anisotropy forcing serious treatment deals with the rutile – type structure anisotropy.

Let me remind after authors [9-11], the two superstructures which are possible in the antiferromagnetic crystals of a rutile – type. In the first structure spins at the corner sites are antiparallel to those at the body center sites, and in the other the corner lattice and the body center lattice are further divided into two antiferromagnetic sublattices. For example, MnF_2 and FeF_2 belong to the superstructure of the 1^{st1} kind (it is not our case), while MnO_2 to that of the 2^{nd2} kind.

Moreover, uranium compound contains two magnetic sublattices, while in the case of scandium sample we face the problem of pseudo-magnetic character one of them (see Fig. 2 upper panel).

The intermetallics described in present paper formed noncollinear alloys. In accordance with unpolarised single crystal neutron data UFe_4Al_8 exhibits commensurate magnetic ordering, i.e. $k_0 = \{0,0,0\}$ while $ScFe_4Al_8$ exhibits flat double modulated structure with magnetic scattering vectors: $k_1 = \{\tau_x, \tau_x, 0\}$ and $k_2 = \{-\tau_x, \tau_x, 0\}$, where $\tau_x = 0.13$ and 0.18 respectively [7]. In the latter case, the magnetic supercell on the level of any elementary cell can be thought of as a superposition of two: non-collinear and collinear ferromagnetic lattices.

In order to construct a map of the exchange integrals reproducing the observed spin ordering, the atomic magnetic moments, magnetic scattering vectors the *MCMag* [12] and *MCPhase* [13] simulation programs were used. Both of them are basing on an algorithm of simulated cooling or heating, see Kirkpatrick [14], while the configuration space is examined by random sampling in accordance with the Metropolis procedure [15]. However, two crucial aspects make both methods different. While *MCPhase* allows finding the exchange integrals J_{ij} by means of a fitting (self-consistent Monte Carlo procedure) and treats the spins quantum-mechanically, much earlier developed *MCMag* treats the spins classically and the exchange constantans have to be guessed.

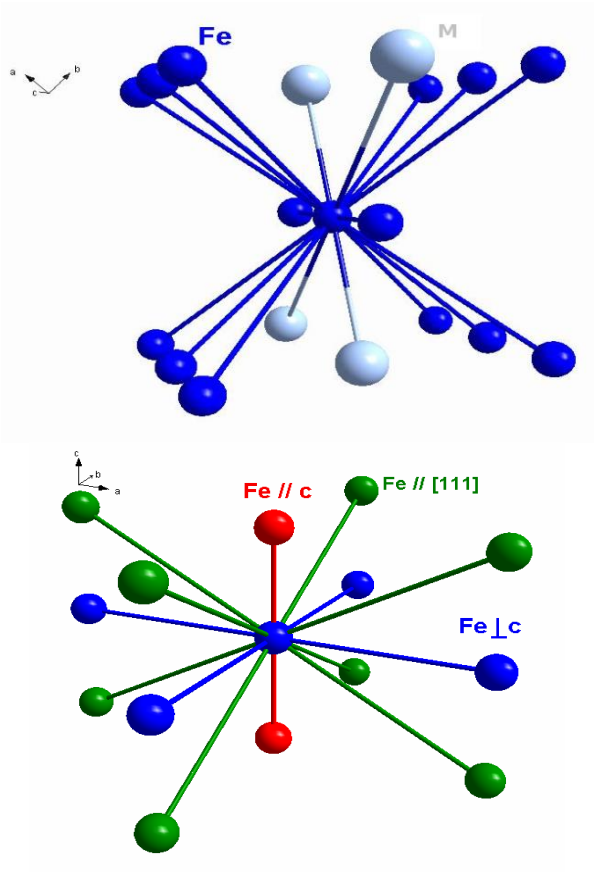

Fig. 2 Nearest neighbors (nn) of mixed type of M and Fe – atoms surrounding an each Fe occupies (8f) positions (upper panel) and anisotropic neighboring of pure Fe origin (lower panel), where the blue neighbors interact with one another by J_{ab} exchange constant, green ones by J_{abc} and the red neighbors exchange interaction by J_{cc} integral.

[1] The anisotropy arises mainly from the magnetic dipole interactions which make the spins parallel to the c axis as the unit cell dimension along the c axis is considerably shorter than that along the a axis.

[2] The magnetic dipole interactions make the direction of the spins perpendicular to the c axis since up and dawn spins line up alternately along this direction and in consequence the crystal lattice is divided into four sublattices, each having parallel spins.

2. Monte Carlo simulation's conditions

To understand what makes the system 3d-3d-3p behaves in such an unconventional manner we can treat the system classically or quantum-mechanically. Therefore, it is convenient to self-consistent both these approaches.

Noteworthy, looking into the Heisenberg interactions there are no origin for the crystal fields or spin – orbital splittings efects typical for rare earth compounds with the general stoichiometry RE:4Fe:8Al. Here, we face the problem of pure or almost pure spin-spin coupling between 3d-3d metals, where the Fe-Fe or Fe-M-Fe interactions should be taken into account only.

Spin only magnetism as a common in the transition metal compounds justifies using Hamiltonian with Heisenberg spins and anisotropic corrections. The comparison of the MC simulation packets leads to a few comments. The starting point of the *MCPhase* calculation is the Hamiltonian: $\mathcal{H} = \mathcal{H}_{cf} + \mathcal{H}_c$ where the crystal field anisotropy is determined by formula $\mathcal{H}_{cf}=\sum_{n,l,m} B_{lm} O_{lm}(J^n)$ and where $\mathcal{H}_c$ takes into account the Coulomb interactions among the electrons and between the electrons and the nucleus. During *MCMag* simulations Hamiltonian takes the form of: $\mathcal{H} = \mathcal{H}_{cf} + \mathcal{H}_{DM}$, where $\mathcal{H}_{cf}=\sum_s {D_z}^2 (J_z)^2 + {K_{xy}}^2 [(J_x)^2 - (J_y)^2]$ and Dzyaloshinskii – Moriya interactions (DM) contributes as $\mathcal{H}_{\mathrm{DM}} = A\vec{n}(\vec{J_1} x \vec{J_2})$.

The simulations start at some high temperature where spins are dynamically disordered. New orientations of spins are drawn at random and adopted or rejected according to Boltzmann statistic. The system escapes from local energy minima and settle in the lowest energy spin configuration. During *MCMag* cycles appropriate agreements factors can be traced: (1) so-called rate of accepted jumps and (2) the constraint function - F_c - which is a measure of the degree of frustration of a magnetic structure. The rate of accepted jumps is the rate of acceptance of new spin configurations at a given temperature and field. Obviously, the rate of accepted jumps takes into account any new spin configuration that is identical to the old one. The constraint function is defined by $-1 \le F_c = -\sum_{<ij>} J_{ij}\vec{S}_i\vec{S}_j / \sum_{<ij>} |J_{ij}||\vec{S}_i||\vec{S}_j| \le 1$ and working in the range from non-frustrated magnetic structures ($F_c = -1$) to totally frustrated one ($F_c = 1$). The treatment of magnetic interactions and spins is purely classical. Any kind of real magnetic structure can be simulated without limitation of interacting distance. The input file contains a list of the magnetic sites of the structure, together with a list of their neighbours and corresponding exchange integrals, as well as anisotropy coefficients and spin amplitudes. No symmetry elements are taken into account.

For convenience, the end of the simulation is the possibility offered by the magnetic moments of the projection of the crystal axis and the rotation of the entire system, so as to put it in a moment in a desired direction of the crystal reference. This option makes it easier to compare the result of simulation and actual or theoretical settings spins. External simulation conditions (cooling protocol, or magnetic scenario) are entered interactively (via dialog boxes). The magnetism of UFe_4Al_8 has been simulated on a sample containing the iron spins lie in the *ab*-plane and the almost antiferromagnetically coupled moments are canted into *b* axis. In order to produce this feature, the positive D_z anisotropy coefficients along *c* and K_{xy} along *b* axes and a negative K_{xy} coefficient along *a* axis had to be assigned. During further tests all of the exchange integrals have been modified up to values possessed from *MCPhase*.

DM interactions, frequently observed in this class of materials [2 – 4], enforces the asymmetric off-diagonal terms, i.e. $J_{ab} = -J_{ba}$. The exchange parameters given in Table 4 can be used to make a prediction for the ordering temperature and the magnetic structure in the ordered state. For simplicity we assume, that the CF anisotropy of iron moments can be described by considering ${D_z}^2 = 0.58$ (*MCMag* and *MCPhase*).

Convergence criterion is to minimize the energy.

Table 1. The magnetic tensors dedicated to (8f) positions of the I4/mmm space group. DM interactions were taking into account.

Exchange tensor	Distance $r_{n'} - r_n$
$\begin{bmatrix} A & A & 0 \\ A & A & 0 \\ 0 & 0 & 0 \end{bmatrix}$	$\begin{pmatrix} 0 \\ 0 \\ \pm c/2 \end{pmatrix}$
$\begin{bmatrix} -B-D & 0 \\ D & C & 0 \\ 0 & 0 & 0 \end{bmatrix}$	$\begin{pmatrix} 0 \\ b/2 \\ 0 \end{pmatrix}$ and $\begin{pmatrix} 0 \\ b/2 \\ \pm c/2 \end{pmatrix}$
	$\begin{pmatrix} 0 \\ -b/2 \\ 0 \end{pmatrix}$ and $\begin{pmatrix} 0 \\ -b/2 \\ \pm c/2 \end{pmatrix}$
$\begin{bmatrix} -E & -G & 0 \\ G & F & 0 \\ 0 & 0 & 0 \end{bmatrix}$	$\begin{pmatrix} a/2 \\ 0 \\ 0 \end{pmatrix}$ and $\begin{pmatrix} a/2 \\ 0 \\ \pm c/2 \end{pmatrix}$
	$\begin{pmatrix} -a/2 \\ 0 \\ 0 \end{pmatrix}$ and $\begin{pmatrix} -a/2 \\ 0 \\ \pm c/2 \end{pmatrix}$
$\begin{bmatrix} -H & -K & 0 \\ K & I & 0 \\ 0 & 0 & 0 \end{bmatrix}$	$\begin{pmatrix} a/2 \\ b/2 \\ 0 \end{pmatrix}$ and $\begin{pmatrix} a/2 \\ b/2 \\ \pm c/2 \end{pmatrix}$
	$\begin{pmatrix} \pm a/2 \\ \mp b/2 \\ 0 \end{pmatrix}$ and $\begin{pmatrix} \mp a/2 \\ \pm b/2 \\ \pm c/2 \end{pmatrix}$

The *MCPhase* fitting programs *searchspace* and *simannfit* are used to cover the parameter space and test different regions of this space for local minima of specific function sta[3](parA, …,parK). The appropriate code are

[3]Standard deviation; If $\exp\left(\frac{sta(newA\ldots)-sta(A\ldots)}{T}\right) < a\ random\ number\ out\ of\ [0,1]$ e step is accepted, but otherwise it is rejected. Several occurriencies N of $sta = \delta_i^2$ contribute to the variance $s^2 = \frac{1}{N}\sum_i \delta_i^2$ which is minimized in the process.

presented in Table 1. Starting at a set of parameter values (par A…) the algorithm [14] changes these values by a randomly chosen step with to (par newA…). The function sta(par newA…) is calculated.

On the basis of the histograms of all contemplated the exchange integrals the sets which lead to a minimum sta value is determined. In order to deal with the interactions a combined mean-field/Monte Carlo algorithm is used in module *mcphas*. For a given temperature and magnetic field vector several possible magnetic structures are stabilized by a mean-field algorithm and the free energy is calculated. From *mcphas* fitting all components of the magnetic moment have to be obtained. The magnetization in the given direction can be used for calculation of the standard deviation sta[4]. Then equal-energetically spin configurations together with a given modulation are calculated. During the calculation a plot of the stabilized magnetic structures and the magnetization is shown on screen.

3. Results and discussion

In order to simplify the discussion of minimizing energy the appropriate phases of all magnetic atoms at magnetic unit cell (listed at 3rd column of Table 2) are shifted by lattice translation vector.

Table 2. Nearest neighbors of Fe_I: (¼, ¼, ¼) where the spin-canted structure with the α - canting angle as well as the collinear and commensurate ferromagnetism of uranium sublattices deal with the experimental results [8] were taken into account.

Atom	Atomic position $\vec{r}$ translated by $\vec{T}=(\frac{1}{4},\frac{1}{4},\frac{1}{4})$	Experimental phase	Appropriate distance with respect to Fe_I $\lvert\vec{r}\rvert(pm)$
UFe_4Al_8			
Fe	I: $(^1/_4,^1/_4,^1/_4)-T=(0,0,0)$	$\varphi_1=\alpha$	0.0
	II: $(^1/_4,^1/_4,^3/_4)-T=(0,0,^1/_2)$		251.51
	III: $(^3/_4,^3/_4,^3/_4)-T=(^1/_2,^1/_2,^1/_2)$		667.0
	IV: $(^3/_4,^3/_4,^1/_4)-T=(^1/_2,^1/_2,0)$		617.76
	V: $(^1/_4,^3/_4,^3/_4)-T=(0,^1/_2,^1/_2)$	$\varphi_2=\pi-\alpha$	504.06
	VI: $(^3/_4,^1/_4,^3/_4)-T=(^1/_2,0,^1/_2)$		504.06
	VII: $(^3/_4,^1/_4,^1/_4)-T=(^1/_2,0,0)$		436.82
	VIII: $(^1/_4,^3/_4,^1/_4)-T=(0,^1/_2,0)$		436.82
U	I: $(0,0,0)-T=-(^1/_4,^1/_4,^1/_4)$	$\varphi_3=\frac{\pi}{2}$	333.5
	II: $(^1/_2,^1/_2,^1/_2)-T=(^1/_4,^1/_4,^1/_4)$		333.5
$ScFe_4Al_8$			
Fe	I	$\varphi_1=\alpha+\pi\tau$	0.0
	II		249.9
	III	$\varphi_2=\alpha+3\pi\tau$	657.6
	IV		608.26
	V	$\varphi_3=\pi-\alpha+2\pi\tau$	497.43
	VI		497.43
	VII		430.1
	VIII		430.1
Sc	I	$\varphi_4=\frac{\pi}{2}$	328.8
	II		328.8

The similar table which was presented for $ScFe_4Al_8$ [16] allows to compare the conditions of minimizing energy, which are presented below. *MCPhase* programs were used to find the exchange parameters Hamiltonian the exchange interactions J^{RKKY}_{Fe-Fe} and J^{RKKY}_{U-Fe} as well as J^{RKKY}_{U-U} with $k_F=0.5$ Å^{-1} were considered.

Taking into account 8 nn, we face the problem of minimizing energy which in the case of noncollinear and incommensurate structure is described by formula:

$$E=-6S_{Fe}{}^2\{J_{aa}cos(\varphi_3-\varphi_1)+J_{aa}cos(\varphi_3-2\pi\tau-\varphi_1)+J_{bb}cos(\varphi_3-\varphi_1)+J_{bb}cos(\varphi_3-2\pi\tau-\varphi_1)+2J_{cc}\}-7S_{Fe}{}^2\{J_{ab}cos(\varphi_2-\varphi_1)+J_{\overline{ab}}cos(\varphi_2-2\pi\tau-\varphi_1)+J_{a\bar{b}}+J_{\bar{a}b}+2J_{ac}cos(\varphi_3-\varphi_1)+2J_{ac}cos(\varphi_3-2\pi\tau-\varphi_1)+2J_{bc}cos(\varphi_3-\varphi_1)+2J_{bc}cos(\varphi_3-2\pi\tau-\varphi_1)\}-4S_{Fe}S_{Sc}\{J_{abc}cos(\varphi_4-\varphi_1)+J_{\overline{abc}}cos(\varphi_4-\varphi_2)+(J_{a\bar{b}c}+J_{\bar{a}bc})cos(\varphi_4-\varphi_3)\} \quad (1)$$

which for the commensurate structure simplifies to:

[4]The standard deviation is calculated as: $sta=\sum_{datapointsi}\left(m_i^{calc}-m_i^{meas}\right)^2$.

$$E = -6S_{Fe}{}^2\{2J_{aa}cos(\varphi_2 - \varphi_1) + 2J_{bb}cos(\varphi_2 - \varphi_1) + 2J_{cc}\} - 7S_{Fe}{}^2\{4J_{ab} + 8J_{ac}cos(\varphi_2 - \varphi_1)\} - 4S_{Fe}S_U\{(J_{abc} + J_{\bar{a}\bar{b}c})cos(\varphi_3 - \varphi_1) + (J_{a\bar{b}c} + J_{\bar{a}bc})cos(\varphi_3 - \varphi_2)\} \quad (2)$$

due to
$J_{ab} = J_{\bar{a}\bar{b}} = J_{a\bar{b}} = J_{\bar{a}b}$ and $J_{ac} = J_{a\bar{c}} = J_{bc} = J_{b\bar{c}}$,
$J_{abc} = J_{\bar{a}\bar{b}c} = J_{a\bar{b}c} = J_{\bar{a}bc}$

thus,
$$E = -6S_{Fe}{}^2\{(2J_{aa} + 2J_{bb})cos(\pi - 2\alpha) + 2J_{cc}\} - 7S_{Fe}{}^2\{4J_{ab} + 8J_{ac}cos(\pi - 2\alpha)\} - 4S_{Fe}S_U\left\{(J_{abc} + J_{\bar{a}\bar{b}c})cos\left(\frac{\pi}{2} - \alpha\right) + (J_{a\bar{b}c} + J_{\bar{a}bc})cos\left(\alpha - \frac{\pi}{2}\right)\right\} \quad (2a)$$

and
$$E = -12S_{Fe}{}^2[(J_{aa} + J_{bb})cos(\pi - 2\alpha) + J_{cc}] - 28S_{Fe}{}^2[J_{ab} + 2J_{ac}cos(\pi - 2\alpha)] - 16S_{Fe}S_U J_{abc}sin\alpha = -12S_{Fe}{}^2[J_{cc} - (J_{aa} + J_{bb})cos2\alpha] - 28S_{Fe}{}^2[J_{ab} - 2J_{ac}cos2\alpha] - 16S_{Fe}S_U J_{abc}sin\alpha \quad (2b)$$

$$\partial E/\partial\alpha = -24S_{Fe}{}^2(J_{aa} + J_{bb})sin2\alpha - 112S_{Fe}{}^2J_{ac}sin2\alpha - 16S_{Fe}S_U J_{abc}cos\alpha \quad (3)$$

Next the conditions for energy minima determine noncollinearity of the magnetic structure:

$$\partial E/\partial\alpha = 0 \Longrightarrow -S_{Fe}sin\alpha\,[3(J_{aa} + J_{bb}) + 14J_{ac}] = S_U J_{abc} \quad (4)$$

thus

$$\frac{S_U}{S_{Fe}} = -\frac{[3(J_{aa} + J_{bb}) + 14J_{ac}]sin\alpha}{J_{abc}} \quad (5)$$

so

$$3(J_{aa} + J_{bb}) + 14J_{ac} = -\frac{S_U J_{abc}}{S_{Fe}sin\alpha} \quad (5a)$$

and
$$\partial^2 E/\partial\alpha^2 = -48S_{Fe}{}^2(J_{aa} + J_{bb})cos2\alpha - 224J_{ac}cos2\alpha + 16S_{Fe}S_U J_{abc}sin\alpha > 0 \quad (6)$$

finally,

$$S_{Fe}[3(J_{aa} + J_{bb}) + 14J_{ac}]cos2\alpha < S_U J_{abc}sin\alpha \quad (7)$$

and

$$\frac{[3(J_{aa} + J_{bb}) + 14J_{ac}]cos2\alpha}{J_{abc}sin\alpha} < \frac{S_U}{S_{Fe}} \quad (8)$$

Taking into account both conditions leading to minimum energy (eqs. 5a and 8) the common solution corresponds to relation:

$$\frac{\left[-\frac{S_U J_{abc}}{S_{Fe}sin\alpha}\right]cos2\alpha}{J_{abc}sin\alpha} < \frac{S_U}{S_{Fe}} \quad (9)$$

$$cos2\alpha < sin^2\alpha \quad (9a)$$

Thus the stable UFe_4Al_8 spin-canted structure is predicted for canting angles $^{\pi}/_{5} < \alpha \leq {}^{\pi}/_{2}$ and from eq. (5a) finally can be obtain relation:

$$J_{aa} + J_{bb} = -5\left(\frac{J_{abc}}{8}\frac{S_U}{S_{Fe}} + J_{ac}\right) \quad (10)$$

Above conditions are weakly consistent with the experimental results [8], where $\alpha \leq {}^{\pi}/_{6}$ was reported. On the other hand, the strongest in-phase scattering was observed along diagonals what leads to prediction of the positive signs of J_{ac}, J_{abc} thus $J_{aa} = -J_{bb}$ is the only consistent condition and undoubtedly resulted in DM-type anisotropy.

A similar approach to obtain the basic relations between exchange constants has been made for $ScFe_4Al_8$ [16]. Obviously, due to conditional solutions of the exchange constants without extra dependences presented here equations are too complicated and it can only resolve them by use Monte Carlo methods.

Table 3. The correlation functions and static magnetic properties: (da=0.25 a db=0.25 b dc=0.25 c) T = 50 [K] H=0 [T] calculated by use MCPhas program, where the exchange constants are expressed in meV.

Correlation Function	$<J_a J_a>$	$<J_b J_b>$	$<J_c J_c>$ e-08	$<J_a J_b>$	$<J_b J_a>$
<JJ(0 0 0.5>	-0.8027	2.651	-0.15	0.7659	-2.779
<JJ(0 0 -0.5>	-0.8027	2.651	-0.15	0.7659	-2.779
<JJ(0 0.5 0 >	-0.924	2.125	-0.7	0.6139	-3.199
<JJ(0.5 0 0 >	-0.924	2.125	-0.7	0.6139	-3.199
<JJ(0 -0.5 0 >	-0.924	2.125	-0.7	0.6139	-3.199
<JJ(-0.5 0 0 >	-0.9244	2.123	-0.7	0.6132	-3.2
<JJ(-0.5 0 -0.5>	-0.9552	1.952	-1.38	0.5639	-3.307
<JJ(0 -0.5 -0.5>	-0.9551	1.953	-1.38	0.564	-3.306
<JJ(0 0.5 0.5>	-0.9551	1.953	-1.38	0.564	-3.306
<JJ(0.5 0 0.5>	-0.9552	1.952	-1.38	0.5639	-3.307
<JJ(-0.5 0 0.5>	-0.9552	1.952	-1.38	0.5639	-3.307
<JJ(0 -0.5 0.5>	-0.9551	1.953	-1.38	0.564	-3.306
<JJ(0 0.5 -0.5>	-0.9551	1.953	-1.38	0.564	-3.306
<JJ(0.5 0 -0.5>	-0.9552	1.952	-1.38	0.5639	-3.307

Not all, but most significant terms of correlation functions were presented above. The residual ones are of less importance. The strong anisotropy manifests itself clearly in the non-equivalence of the terms listed at columns 5th and 6th of Table 3.

MCMag is an appropriate tool for simulation of the magnetic structure when coupling constants are known or can be roughly estimated. By similarity tocanting structure of the rutile (MnO_2), the appropriate exchange integrals (-

0.7586 meV//a, 0.4741 meV//b conditions only, assuming coupling constant values and -0.1121meV//c) [17] were implemented into tested magnetic models. The magnetic structure of UFe_4Al_8 has been simulated on a sample containing 1x1x1 cells with all directions under periodic listed above. Finally, below mentioned exchange integrals were obtained.

Table 4. The solution of bilinear magnetic tensors dedicated to 6nn of each i-th iron atom located at (8f) positions of the I4/mmm space group, taking into account DM interactions where the appropriate vectors $\vec{r_i} - \vec{r_j}$. The elements of the square matrix are shown in the 3th and 4th column.

Exchange tensor parameters	$(r_i - r_j)/pm$	*MCPhase* J_{ij}*[meV]*	*MCMag* J_{ij}*[meV]*
A	$\begin{pmatrix} 0 \\ 0 \\ \pm 251.5 \end{pmatrix}$	0.46	0.03
$B(-)$	$\begin{pmatrix} 0 \\ 436.8 \\ 0 \end{pmatrix}$	1.14	2.011
C		0.63	1.66
D(±)	$\begin{pmatrix} 0 \\ -436.8 \\ 0 \end{pmatrix}$	1.36	2.111
$E(-)$	$\begin{pmatrix} 436.8 \\ 0 \\ 0 \end{pmatrix}$	0.98	1.31
F		0.99	1.05
G(±)	$\begin{pmatrix} -436.8 \\ 0 \\ 0 \end{pmatrix}$	1.19	1.54

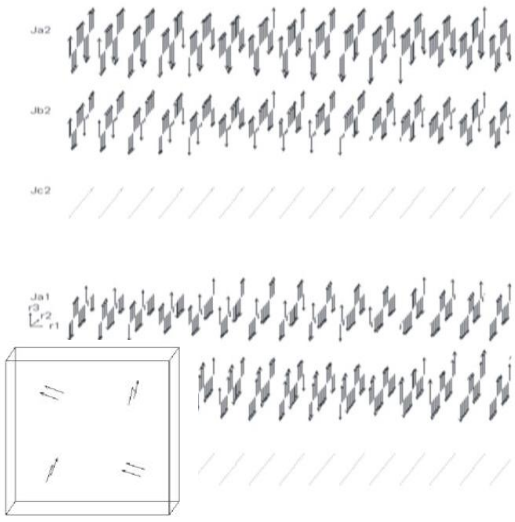

Fig. 3 Configuration projections of the exchange integrals JJ of 225 spins which form magnetic unit cell of $ScFe_4Al_8$ alloy with scattering vector $k_{1,2} = \{\pm 0.13, 0, 13, 0\}$ and the total iron magnetic moment equal to μFe = 1.46 μ_B (upper and middle panels) and [001] projection of the 8 spins which form commensurate magnetic unit cell of UFe_4Al_8 with μFe = 0.87μ_B (lowest panel) obtained by MCPhase at T=41 K.

Moreover, according to neutron data results [8] and for better visualization the iron spin rearrangement at the temperatures above 50 K the 3a x 3a x c magnetic supercell of incommensurate scandium structure [16] has been recalled in Fig. 4. The magnetic ordering of the uranium sample reproduces itself correctly at 231 or 321 cells.

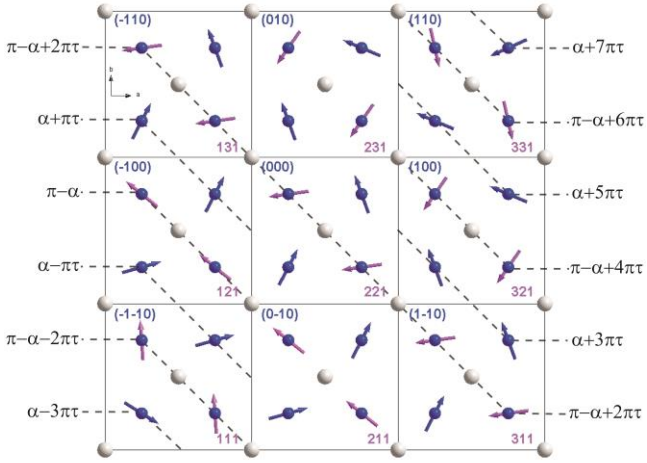

Fig. 4 2D schematic representation of the iron moment arrangement in the ab plane containing the wave vector $(\tau_i, \tau_i, 0)$ which locks-in to $(0,0,0)$ at 231 or 321 cells, respectively.

4. Remarks and conclusions

By use of both programs we are able to reconstruct more or less correctly the magnetic structures of MFe_4Al_8 experimentally confirmed. Two significant differences in the model assumptions should be emphasized: (1) different formulas of the Hamiltonian equations and (2) much more detail characteristic of the single ion anisotropy and possibility of use the isoelectronic configurations, i.e. Ni^{2+} instead of Fe^0 and V^{2+}instead of Sc^0 or to choose U^{3+} ($5f^3$) instead of U^{4+}($5f^2$) in the case of *MCPhase* program.

So far, trying to reproduce the spin arrangement based on the exchange integrals and phase transition temperature in the case of the structure of a single modulation leads to success. Consistently to experimental results the solution of the resultant magnetic moments of the iron atom ~ 0.9 μ_B, is obtained. In the case of appropriate ratios of the exchange constants the agreement seems to be worse: $-1.2_{MCMag} > \frac{J_{aa}}{J_{bb}} > -1.8_{MCPhase}$ and $-67_{MCMag} < \frac{J_{aa}}{J_{cc}} < -2.5_{MCPhase}$. Noteworthy, the highly correlated states of *5f* electrons in metallic actinide compounds are not the states of single electrons. The intra-atomic Coulomb, spin-orbit and crystal-field interactions are probably as large or larger then than the *f-f* or *d-f* interatomic hopping energies. In such a case, it is reasonable to begin with fully localized or crystal-field description of the *f* states and then to add the hopping energies leading to same degree of itinerant motion. In the metallic actinides, the signs and magnitudes of the crystal-field parameters are unknown. Moreover, the crystal-field ground state of the $5f^2$ configuration is normally found to

be the nonmagnetic singlet. To verify all above disagreements, inelastic neutron scattering on single crystals and *ab-inito* calculations of phonon dispersion would be desirable.

References

[1] P. Schobinger-Papamantellos, K. H. J. Buschow, C. Ritter, J. Magn. Magn. Mat. **186** 21 (1998).

[2] W. Sikora, P. Schobinger-Papamantellos, K.H.J. Buschow, J. Magn. Magn. Mat. **213** 143 (2000).

[3] J.A. Paixão, M.R. Silva, J.C. Waerenborgh, A.P. Gonçalves, G.H. Lander, P.J. Brown, M. Godinho, P. Burlet, Phys. Rev. B **63** 054410 (2001).

[4] K. Rećko, L. Dobrzyński, K. Szymański, D. Satuła, K. Perzyńska, M. Biernacka, J. Waliszewski, P. Zaleski, W. Suski, K. Wochowski, M. Hofmann D. Hohlwein, Phys. Stat. Sol. A **196** 344 (2003).

[5] M. Bacmann, Ch. Baudelet, D. Fruchart, D. Gignoux, E.K. Hlil, G. Krill, M. Morales, R. Vert, P. Wolfers, J. Alloys Comp. **383** 166 (2004).

[6] W. Suski, J. Alloys Comp. **223** 237 (1995).

[7] K. Rećko, L. Dobrzyński, A. Goukassov, M. Biernacka, M. Brancewicz, A. Makal, K. Woźniak, J. Waliszewski, E. Talik, B. Yu. Kotur, W. Suski, Phase Transit. **80** 6-7 575 (2007).

[8] K. Rećko, M. Biernacka, L. Dobrzyński, K. Perzyńska, D. Satuła, J. Waliszewski, W. Suski, K. Wochowski, G. André, F. Bourée, J. Phys. Cond. Matter **9** 9541 (1997).

[9] P. W. Anderson, Phys. Rev. **79**, 705(1950).

[10] J. H. Van Vleck, J. de Phys. et Radium **12,** 262 (1951).

[11] R. A. Erickson and C. G. Shull, Phys. Rev. SiS 208 (1951).

[12] P. Lacorre and J. Pannetier, J. Magn. Magn. Mat. **71** 63 (1987).

[13] M. Rotter and DucManh Le: http://www.mcphase.de

[14] S.Kirkpatrick, C.D. Gelatt and M.P. Vecchi, Science **220** 671 (1983).

[15] N. Metropolis, A. Rosenbluth, M. Rosenbluth, A. Teller, E. Teller, J. Chem. Phys. **21** 1087 (1953).

[16] K. Rećko, L. Dobrzyński, J. Waliszewski, K. Szymański, Acta Physica Polonica A **127**(2), 424 (2015).

[17] O. Nabuhiko, H. Yoshikazu, J. Phys. Soc. Jpn. **30** 1311 (1971).

*Corresponding author: k.recko@uwb.edu.pl